Molecular Vision 2018; 24:367-378 <http://www.molvis.org/molvis/v24/367>
Received 28 March 2017 | Accepted 16 May 2018 | Published 18 May 2018

Low-dose minocycline mediated neuroprotection on retinal ischemia-reperfusion injury of mice

Ruojing Huang,[1] Shaomin Liang,[1] Lyujie Fang,[1] Min Wu,[4] Huanhuan Cheng,[5] Xuesong Mi,[1,2,3] Yong Ding[1]

(The first two authors contributed equally to the work)

[1]Department of Ophthalmology, The First Affiliated Hospital of Jinan University, Guangzhou, China; [2]Changsha Academician Expert Workstation, Aier Eye Hospital Group, Changsha, China; [3]School of Optometry, The Hong Kong Polytechnic University, Hung Hom, Hong Kong; [4]Department of Ophthalmology, Guangzhou first people's hospital, Guangzhou, China; [5]Department of Ophthalmology,The third Affiliated Hospital, Sun YAT-SEN University

Purpose: The aim of this study was to investigate the effect of minocycline (MC) on the survival of retinal ganglion cells (RGCs) in an ischemic-reperfusion (I/R) injury model of retinal degeneration.
Methods: Retinal I/R injury was induced in the left eye of mice for 60 min by maintaining intraocular pressure at 90 mmHg. Low- or high-dose MC (20 or 100 mg/kg, respectively) was administered by intravenous injection at 5 min after the retinal ischemic insult and then administered once daily until the mice were euthanized. RGCs and microglial cells were counted using immunofluorescence staining. Functional changes in the RGCs were evaluated using electroretinography. The visual function was assessed using an optokinetic test.
Results: The data demonstrated that the effect of MC was dose dependent. Low-dose MC showed protective effects, with reduced RGC loss and microglial activation, while the high-dose MC showed damage effects, with more RGC loss and microglial activation when compared with the vehicle group. The electroretinography and optokinetic test results were consistent with the morphologic observations.
Conclusions: These data suggested that appropriate concentrations of MC can protect the retina against retinal ischemic-reperfusion injury, while excessive MC has detrimental effects.

Retinal ischemia is an important pathomechanism within various retinal degenerative diseases, such as glaucoma, diabetic retinopathy, and retinal artery occlusion [1]. Glaucoma, characterized by retinal ganglion cell (RGC) death, is a global disease and can lead to irreversible blindness [2]. Although elevated intraocular pressure (IOP) is a major causative factor in glaucoma, additional factors are involved in its pathogenesis [3]. Other than lowering IOP, novel strategies aiming to inhibit glaucomatous neurodegeneration are important [4]. Therapies that delay or halt the loss of RGCs have been proved to be effective in preserving the vision of patients with glaucoma [5]. During the progressive loss of RGCs, structural and functional changes in the retina have been identified in previous studies [6,7]. The ocular hypertension-induced retinal ischemic-reperfusion injury model has been frequently used to investigate the pathogenesis of RGC death and explore new neuroprotective therapies to inhibit the ischemic damage of glaucoma [8,9].

Minocycline (MC) has been found to have neuroprotective effects in diseases of the central nervous system (CNS) [10,11], such as middle cerebral artery occlusion [12,13], Alzheimer disease [14], Parkinson disease [15], oxygen–glucose deprivation [16], and Huntington's disease [17]. Growing evidence also showed that minocycline likely has a neurologic effect in many retinal diseases [18,19]. A study of retinal ischemia-reperfusion injury reported that minocycline exerted a neuroprotective effect through preventing retinal inflammation and vascular permeability [20]. Minocycline has also been used as an antioxidant agent to prevent retinal disease [21,22]; another important function of minocycline is suppression of microglial activation in neurologic diseases [23-25]. These studies support the idea that minocycline has a neuroprotective role. However, it was reported that minocycline could exacerbate visual dysfunction in a mouse model of retinopathy of prematurity (ROP) [26]. In short, the role of minocycline in the treatment of neurologic retinal diseases is contradictory with the mechanism still unknown. Microglial cells are a major type of immune cells in the CNS and have been thought to be involved in the pathogenesis of glaucoma [27,28]. Activated microglia are inflammatory cells and are detrimental to the function of the CNS [29]. It has been reported that microglial cells have diverse phenotypes and can rapidly transform into the reactive state in response to various insults [30]. A recent study showed that MC could

Correspondence to: Xuesong Mi, Department of Ophthalmology, The First Affiliated Hospital of Jinan University, Guangzhou, China; Phone: 13416147928; FAX: 020-38688397; email: mxsong@163.com

reduce photoreceptor damage by suppressing the activation of microglia in retinitis pigmentosa [23]. Moreover, it has been reported that there is a loss of photoreceptors in glaucoma [31,32]. However, no study has investigated the functional change in RGCs under the treatment of MC in the ischemic retina. In the present study, we used molecular biology and visual function tests to determine whether MC could prevent the degeneration of RGCs in retinal ischemic insult and confirmed that MC is a promising therapeutic agent in models of neurologic ischemic damage.

METHODS

Animals: C57BL/6 male mice (8–12 weeks, weight approximately 20–25 g; purchased from Guangdong Medical Laboratory Animal Center) were used in the study. They were housed in a 12 h:12 h light-dark cycle and allowed free access to food and water. All experimental designs and protocols were conducted according to the recommendations of the National Institutes of Health *Guide for the Care and Use of Laboratory Animals* and were approved by the Jinan University Institutional Animal Care and Use Committee.

Retinal ischemia-reperfusion injury model: Mice were anesthetized with an intraperitoneal injection of 2.5% tribromoethanol. Before the eye surgery, the pupil was dilated with one drop of 0.5% tropicamide for 5 min, and then the cornea was desensitized with one drop of 0.4% oxybuprocaine hydrochloride eye drops. The ischemia-reperfusion (I/R) injury model was induced by inserting a 33 G needle into the anterior chamber of the left eye. A reservoir of normal saline (of 0.9%) was linked to the needle and hung up to maintain the IOP at 90 mmHg for 60 min (monitored with TonoLab, U.S. Pat. 6,093,147). After the surgery, 0.3% tobramycin was administered in the conjunctival sac to prevent inflammation.

Drug administration: The mice were randomly divided into four experimental groups: the control group, the I/R injury + normal saline (NS) group, the I/R injury + low-dose MC group, and the I/R injury + high-dose MC group. First, to test the effective low dosage, five animals in each group received 10, 20, or 30 mg/kg MC, respectively, via intravenous injection. The RGCs were counted to estimate the effect of MC. Further, two groups of five animals received either 80 or 100 mg/kg MC intravenously to obtain the effectiveness of high-dose MC. Finally, based on the results, the low dose of 20 mg/kg MC was confirmed and administered via the caudal vein 5 min after the operation and once per day until the animals were euthanized with intraperitoneal injection of 2.5% tribromoethanol anesthesia. while 100 mg/kg MC was used for the high-dose group as previously reported [33]. The mice received a volume of 0.1 ml solution of MC per 10 g bodyweight. Mice in the I/R injury + NS group were treated with an equal volume of NS.

Histology: Mice were anaesthetized using 2.5% tribromoethanol. Perfusion–fixation was performed with 0.9% NS until bleed out, followed by 4% paraformaldehyde in PBS (0.1 M; 8.6 g Nacl, 2.68 g NaH_2PO_4, 11.51 g Na_2HPO_4, pH 7.4) until the tissues stiffened. The enucleated eyeball cup was trimmed and immediately fixed in 4% paraformaldehyde for 1 day at 4 °C, followed by dehydration with 30% sucrose solution overnight, and embedded in a compound Tissue Freezing Medium (SAKURA4583, Tissue-Tek OCT, American; Torrance, CA) at –20 °C. The eye tissues were cut horizontally at 10 µm thick using a microtome (RM2235, Leica, Wetzlar, Germany). Four nonconsecutive sections through the optic nerve were used from each mouse under the same conditions. Hematoxylin and eosin (H&E) staining was used on the retinal sections to evaluate the inner retinal layer (IRL), which was measured from the inner limiting membrane to the inner nuclear layer. Images were taken using a Leica light microscope. For statistical analysis, retinal thickness was measured at the middle retina at 1.1 mm on both sides from the optic nerve head [11].

Immunofluorescence: First, flat-mounted retinas were fixed in 4% paraformaldehyde overnight. The orientation of each eye was carefully marked with a nick on the nasal side during dissection. Tissues for immunofluorescence were then rinsed with PBS, followed by blocking in PBS with 0.3% Triton X-100 and 10% goat serum for 1 h at room temperature. They were then incubated with primary antibody diluted in blocking solution overnight at 4 °C. The primary antibodies used in this study included goat anti-Brn3a (1:400; Santa Cruz Biotechnology, Santa Cruz, CA) and rabbit anti-Iba1 (1:600; Wako, Osaka, Japan) [34,35]. After rinsing in PBS, the retinas were incubated with secondary antibodies at room temperature for 3 h, followed by rinsing again with PBS. After that, the retinal flat-mounts were mounted on the slide and sealed with an antiquenching reagent and the coverslip. Finally, the retinas were observed, and photographs were taken using a fluorescence microscope (DM6000B, Leica).

Optokinetic test: The optokinetic test (OKT) was performed to assess the visual acuity of the animals [36]. Briefly, each animal was placed freely on a platform in the center of a chamber. The observer operated the software on a desktop computer, which automatically changed the gratings until a reliable threshold was reached. The whole experiment was conducted in a quiet and dark room maintained at a suitable temperature and low noise level to achieve the best responses. In this study, the OKT was conducted at day 4 after the I/R insult. The spatial frequencies tested in the study were 0.05,

0.06, 0.07, 0.1, 0.15, 0.2, 0.25, 0.30, and 0.35 cycles per degree (cpd). Clockwise drifting grates were used to determine the visual function of the left eye, and counterclockwise drifting grates were used for the right eye. The observer judged "Yes" or "No" depending on whether the animal's neck moved along with the drifting scene. The final OKT score was obtained as the highest frequency of grating record which was just before the observer selected the first "No" [37,38].

Electroretinography: Electroretinography (ERG) is used to evaluate the electrical activities and function of signals in different types of retinal cells. In this study, ERG was performed 7 days after the I/R insult using the protocols described previously [39-41]. The mice were prepared for ERG recording after overnight dark adaption. The animals were then anesthetized, and the pupils were dilated, followed by lubricating with 1% methylcellulose. Each animal was placed on a homeothermic device at 37 °C. Recording electrodes of gold wire loop were placed on the cornea. Two reference electrodes were inserted into the subdermis between the ears, while another electrode inserted into the tail acted as a ground. The a-wave, b-wave, and photopic negative response (PhNR) were recorded using the Roland Consult (Brandenburg, Germany) electrophysiological diagnostic system. Light intensities were adjusted as standard luminance intensity units in candela seconds per meter squared (cd.s/m^2). Scotopic ERGs were recorded after dark adaptation with intensities of 3 cd.s/m^2. After that, light adaption under the continuous white background of 25 cd.s/m^2 was applied for 10 min to suppress rod-cell photosensitivity, and the PhNR was recorded using the white flashes of 3 cd.s/m^2. A-waves produced by photoreceptors were measured from the baseline to the first negative peak. B-waves conducted by the ON bipolar cells were measured from the trough of the a-wave to the subsequent positive peak. The PhNR was derived from RGCs and is the negative peak following the b-wave [42].

Statistics: All data were analyzed using the statistical software program GraphPad version 5.0 (GraphPad Software, San Diego, CA) and were presented as means ± standard error of the mean. One-way ANOVA followed by the Newman-Keuls multiple comparison test was used for quantitative analysis, and the Kruskal–Wallis test followed by Dunn's multiple comparison tests were used for qualitative analysis. A p value of less than 0.05 was considered statistically significant. The ERG waves were analyzed using RETI-port software (Roland Consult) after 50 Hz low-pass filtering was applied.

RESULTS

Low-dose MC reduced RGC loss in the mouse I/R injury model: To detect the dose effect of MC, the number of RGCs was counted at day 4 post-I/R injury using Brn3a immunostaining among the different groups. The RGC numbers were averaged from four quadrants of the whole-mounted retina by using five grids of 160 × 160 μm^2 from the optic disc to the border at 500-μm intervals (Figure 1A,B). There was no statistically significant difference in the number of RGCs between the group that received 10 mg/kg MC (2,332±86.39/mm^2) and the I/R injury + NS group (2,125±99.68/mm^2). However, a higher number of RGCs was observed in the 20 mg/kg MC group (2,511±75.17/mm^2) and the 30 mg/kg MC group (2,569±74.32/mm^2), while a lower number was observed in the 80 mg/kg MC group (2,069±75.09/mm^2) and the 100 mg/kg MC group (1,825±79.08/mm^2; all groups, n=5). Other than the 10 mg/kg MC group and the 80 mg/kg MC group, there was a statistically significant difference when compared with the I/R injury + NS group ($p<0.05$). Finally, in the experiments, the optimal low dose of MC was 20 mg/kg, and the lowest harmful high dose of MC was 100 mg/kg (Figure 1C).

There was an approximately 33% reduction in the number of RGCs in the I/R injury + NS group (Figure 1E, n=7) compared with the control group (Figure 1D, n=7; 2,023±95.24 versus 3,192±99.1/mm^2, $p<0.001$). This detrimental effect of I/R injury was markedly alleviated with the administration of low-dose MC (2,432±74.73/mm^2, $p<0.01$; Figure 1F, n=7) but was aggravated by high-dose MC (1,732±82.48/mm^2, $p<0.05$; Figure 1G, n=7). Treatment with low-dose MC reduced the loss of RGCs (by 23±2.3%), whereas high-dose MC worsened the loss of RGCs (by 45±2.5%; Figure 1H,I).

The thickness of the IRL was evaluated by using H&E staining (Figure 2) on day 7 after the I/R insult. Quantitative analysis showed there was a statistically significant difference in the thickness of the IRL between the control group (104±2.40 μm; Figure 2A) and the I/R injury + NS group (55±2.2 μm; Figure 2B). The IRL was thicker in the low-dose MC group (75±2.2 μm; Figure 2C) compared with the I/R injury + NS group, whereas there was no obvious difference between the high-dose MC group (54±5.1 μm; Figure 2D) and the I/R injury + NS group. Thus, we found that the detrimental effect of the I/R insult was alleviated by treatment with low-dose MC (20 mg/kg).

Low-dose MC reduced the activation of microglial cells in the I/R injury model: The number of microglia was quantified based on the standard that resting microglial cells have small cell bodies and few, thin processes, while activated

microglial cells are characterized by enlarged cell bodies with numerous hypertrophied processes or amoeboid cell bodies [43]. Microglial cells were counted by scanning the z-axis across the retinal surface in the ganglion cell layer using a 20X objective lens. Four to five grids of 160 × 160 μm^2 were averaged in each quadrant. One observer, who was blinded to the experimental group, calculated the number of microglial cells under the fluorescence microscope.

After 4 days of I/R insult, microglia were identified using anti-Iba1 immunostaining (Figure 3). The numbers of activated Iba1-positive cells were statistically significantly increased in the retinas from the I/R injury + NS group (88.0±4.50/mm^2, n=7; Figure 3B) compared with the control group (11±2.5/mm^2, n=7; Figure 3A). Low-dose MC alleviated microglial activation (53±3.3/mm^2, n=7; Figure 3C) compared with the I/R injury + NS group. Compared with the I/R group, the high-dose MC group statistically significantly aggravated microglial activation (106±4.40/mm^2, n=7; Figure 3D). The results revealed a statistically significant reduction in microglial activation in the low-dose MC-treated retinas compared with the I/R injury + NS group and the high-dose MC-treated group.

Low-dose MC improved optokinetic responses: The OKT is currently a commonly used tool to assess the visual function of animals [44]. Visual stimuli are projected on computer monitors so that a virtual cylinder with vertical sine wave gratings is drawn by the monitors (Figure 4A,B). The cylinder is rotated at 12 degrees per second to elicit each mouse to stop moving its body and track the grating (Figure 4C). The grating frequency is increased when an observer selects

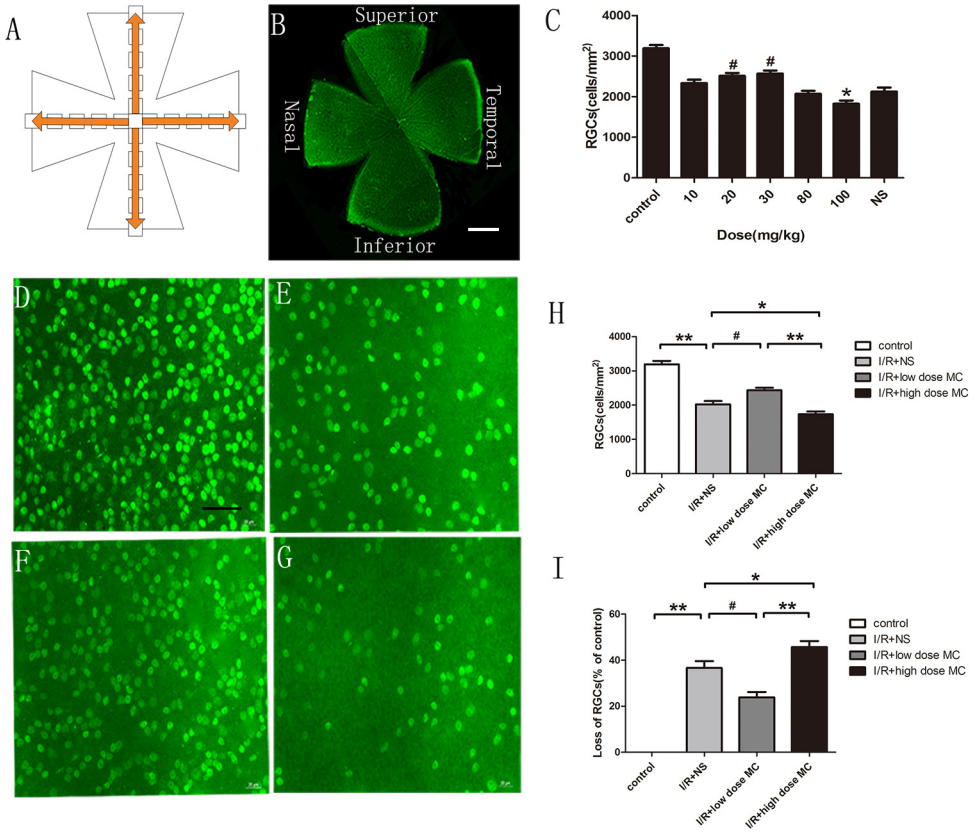

Figure 1. Minocycline treatment reduced RGC loss in the I/R injury retina. **A**: Graphic showing the systemic sampling method used to count the retinal ganglion cells (RGCs). **B**: Whole-mounted retina immunostained with Brn3a antibody. Scale bar = 200 μm. **C**: The effects of test doses of minocycline (MC) on RGCs at day 4 post-ischemic reperfusion (I/R) insult, comparing each dose of MC with the normal saline (NS) vehicle group on the number of RGCs using Brn3a immunostaining (n=5). **D**–**G**: Photomicrographs showing the mid-peripheral area of the retina labeled by Brn3a in the non-I/R injury control group (**D**), the I/R injury + NS vehicle group (**E**), the low-dose MC treatment group (**F**), and the high-dose MC treatment group (**G**). Scale bar = 50 μm. **H**, **I**: Histograms showing the percentage of surviving RGCs and the loss ratio of the RGCs (n=7). *p<0.05, #p<0.01, **p<0.005.

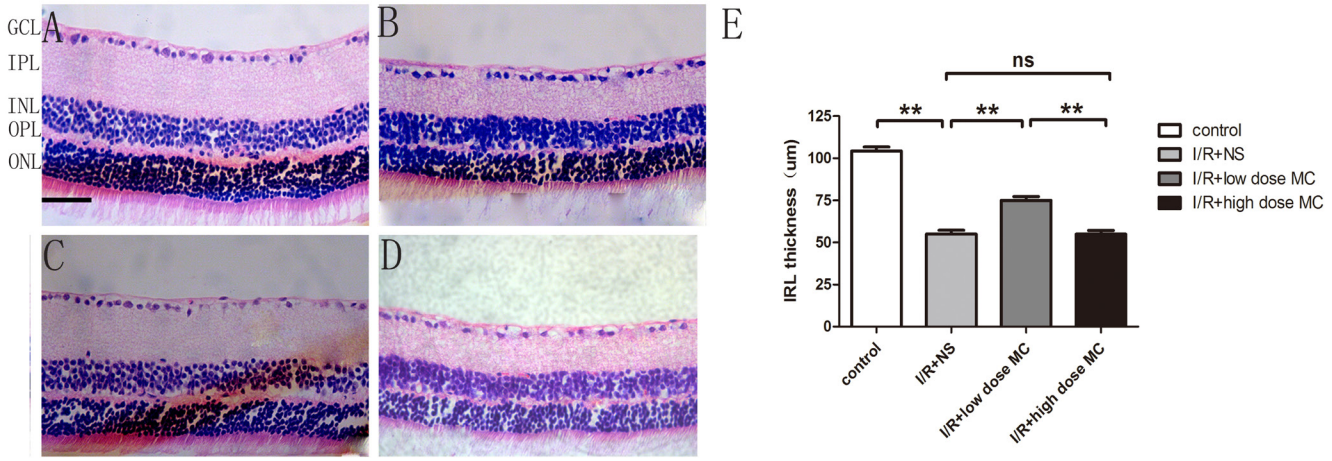

Figure 2. Change in the inner retinal layer in minocycline-treated retinas after retinal ischemic reperfusion injury. **A**–**D**: Photomicrographs demonstrating the hematoxylin and eosin (H&E)-stained retinal section from the middle area in the ischemic-reperfusion (I/R) injury control group (**A**), the I/R injury + normal saline (NS) vehicle group (**B**), the low-dose minocycline (MC) treatment group (**C**), and the high-dose MC treatment group (**D**). Scale bar = 50 µm. **E**: Histogram quantifying the inner retinal layer (IRL) thickness (n=8). **p<0.005.

"Yes," and the system uses a simple staircase method until the mouse shows no visible reaction to the moving gratings (Figure 4D) [45].

Before the I/R insult, there was no difference between the eyes, and both exhibited normal acuity (left: 0.350 cpd; right: 0.350 cpd) in the OKT performed at noon. The OKT responses decreased in the eyes of the I/R injury + NS group (0.156±0.014 cpd, n=8) compared with the control group (0.350 cpd, n=5) on day 4 following the I/R procedure, while the low-dose MC-treated mice (0.218±0.013 cpd, n=8) maintained higher responses than the I/R injury + NS mice (Figure 4E). Meanwhile, the high-dose MC group (0.150±0.013 cpd, n=8) showed no discernible difference compared with the I/R injury + NS group. The data demonstrated that low-dose MC treatment preserved the function of RGCs in the retinas.

MC treatment markedly reversed ERG changes caused by the I/R insult: ERG recordings were performed at scotopic 3 cd s/m^2 and photopic 3 cd s/m^2. ERG recordings for each group are shown in Figure 5. The a-wave, b-wave, and PhNR were recorded (Figure 5A,B). The PhNR amplitudes were reduced in the I/R injury + NS eyes (20.40±1.750 µV, n=15) compared with those for the control eyes (46.80±2.95 µV, n=15). In addition, the PhNR amplitude in the low-dose MC-treated eyes (27.76±1.790 µV, n=15) was markedly higher than in the I/R injury + NS group. The PhNR amplitude was lowest in the high-dose MC group (14.37±1.640 µV, n=15; Figure 5C). The amplitudes of the scotopic ERG a-waves (75±4.0% of baseline values, n=8) and b-waves (60±2.0% of the baseline values, n=8) showed a reduction in the I/R injury + NS mice compared with the eyes of the mice in the untreated normal control group, while the low-dose MC-treated group revealed less reduction in scotopic ERG a-waves (84±3.0% of the baseline values, n=8) and b-waves (66±2.0% of the baseline values, n=8) compared with those for the I/R injury + NS mice (Figure 5D). Under the stimulus of photopic 3 cd s/m^2, the amplitudes of the b-waves were also better preserved in the low-dose MC group (67±2% of the baseline values, n=8) compared with the amplitudes for the I/R injury + NS group (59±3% of the baseline values, n=8). However, the amplitude of the photopic a-waves was not statistically significantly different among these groups (Figure 5E). The latency time of the scotopic ERG a- and b-waves was longer in the I/R injury + NS group (21.3±0.50 and 46.3±1.50 ms, respectively) than in the control group (18.8±0.40 and 41.0±1.20 ms, respectively). The latency time was slightly shorter in the low-dose MC group (a-wave: 19.1±0.40 ms, b-wave: 43.0±1.40 ms) compared with the I/R injury + NS group. In contrast, the PhNR amplitude of the I/R animals treated with high-dose MC (a-wave: 21.5±0.60 ms, b-wave: 48.0±1.30 ms) showed greater reduction than the I/R injury + NS mice, but the latency times were not obviously exacerbated (Figure 5F).

The scotopic ERG results suggested that low-dose MC protected against loss of rod-derived retinal function in I/R insult. However, the latency times of photopic ERG a- and b-waves showed no statistically significant differences among these groups (Figure 5G). Amplitudes of the PhNR were

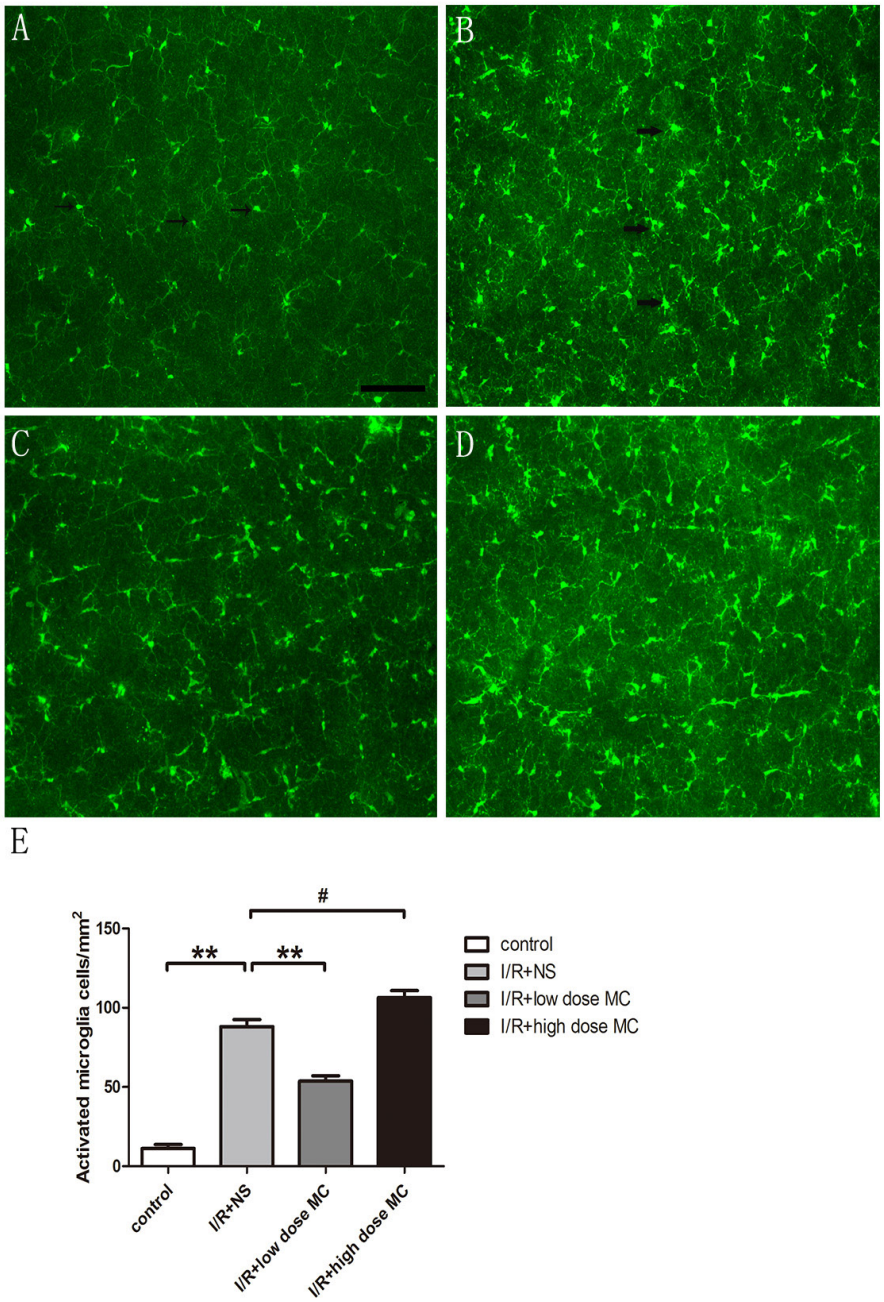

Figure 3. Low-dose minocycline alleviated the activation of microglia in the retinal I/R injury model. The resting microglial cells have small cell bodies and few, thin processes, while activated microglial cells are characterized by enlarged cell bodies with numerous hypertrophied processes or amoeboid cell bodies. **A**–**D**: Whole-mounted retinas showing Iba1-positive microglia throughout the retina in the control group (**A**), with arrows identifying resting microglia, (**B**) the ischemic reperfusion injury (I/R) + normal saline (NS) vehicle group with the arrows identifying activated microglial cells, (**C**) the low-dose minocycline (MC) group, and (**D**) the high-dose MC group. Scale bar = 100 µm. **E**: Quantitative estimate of the numbers of activated Iba1-positive microglia (n=7). $^{\#}p<0.01$,$^{**}p<0.005$.

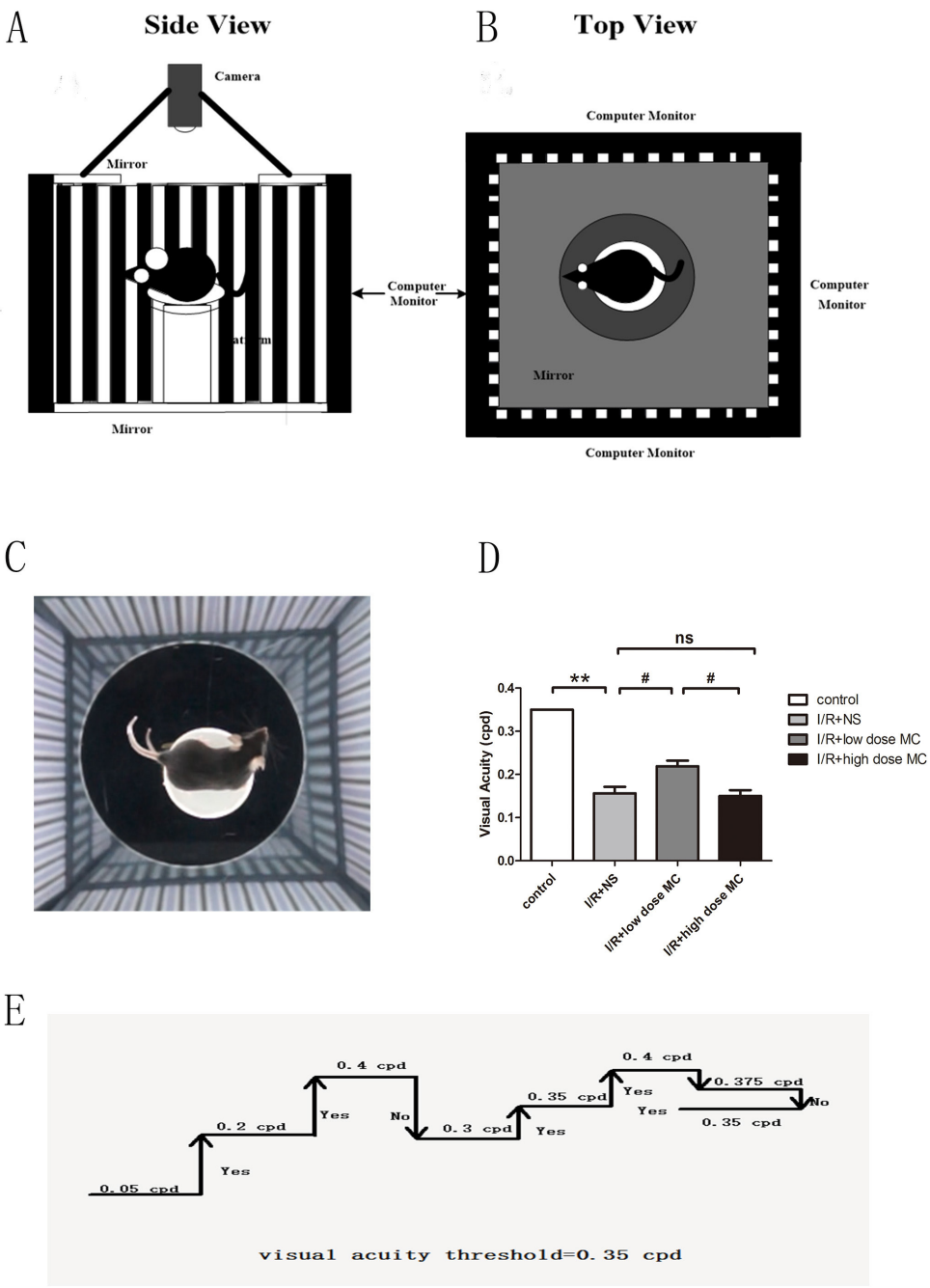

Figure 4. Minocycline (MC) treatment improved optokinetic responses. **A**, **B**: Diagram illustrating the optokinetic testing apparatus. **C**: Video camera image of a mouse tracking the grating. **D**: Simple staircase method of measuring the visual acuity threshold in the optokinetic test (n=8). **E**: Histogram of visual acuity. #p<0.01, **p<0.005.

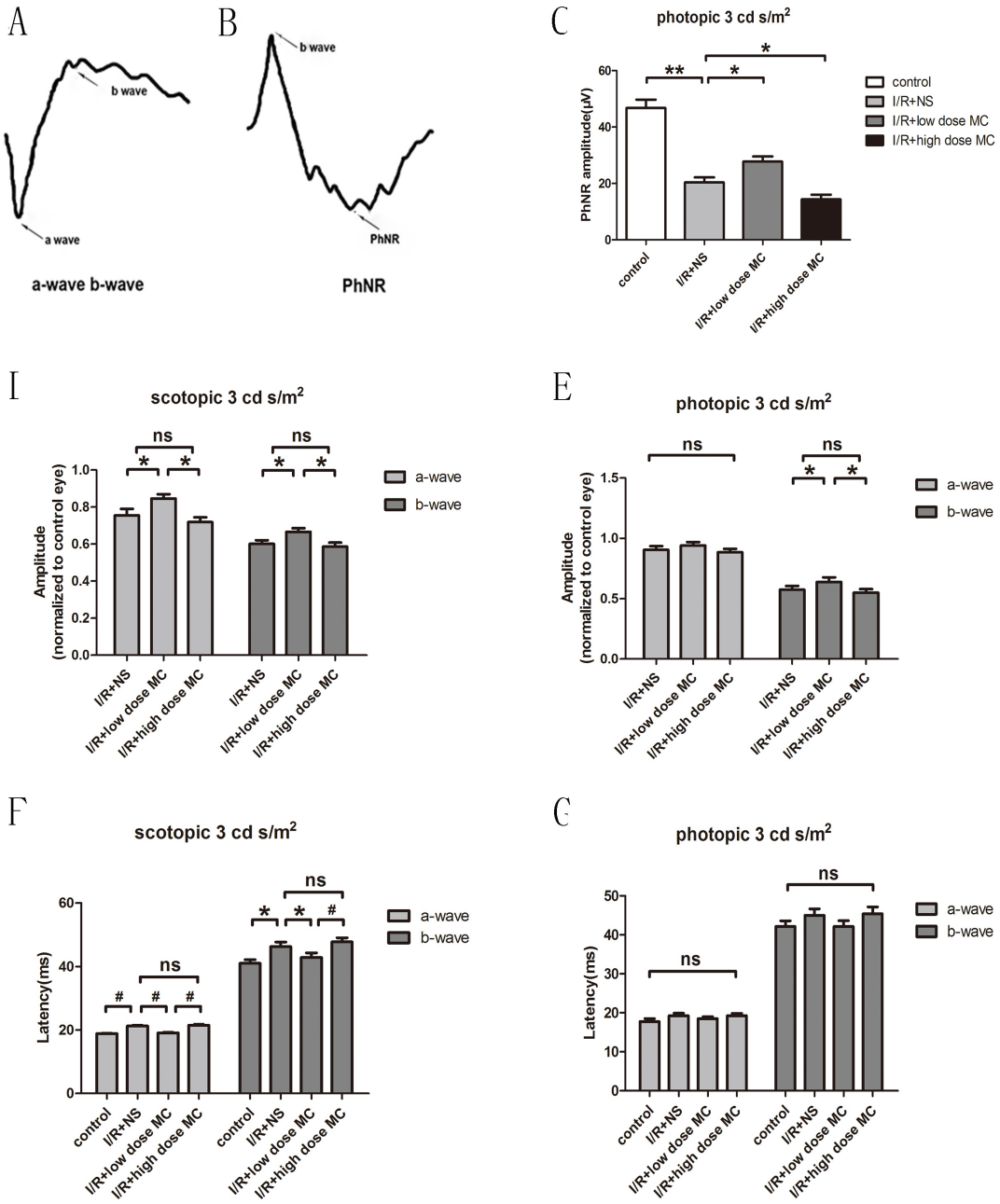

Figure 5. Electroretinography of the different groups before and after the I/R insult. **A**, **B**: Graphic demonstrating the electroretinography (ERG) component (a-wave, b-wave, and photopic-negative response [PhNR]). **C**: PhNR amplitudes at photopic 3 cd s/m^2 (n=15). **D**, **E**: Mean amplitudes of saturated ERG responses, presented as the relative change from the baseline and normalized to a control eye at scotopic 3 cd s/m^2 (**D**) and photopic 3 cd s/m^2 (**E**; n=15). **F**, **G**: Average latency times of ERG a-waves and b-waves at scotopic 3 cd s/m^2 (**F**) and photopic 3 cd s/m^2 (**G**; n=15). *p<0.05, #p<0.01,**p<0.005.

consistent with histological changes and behavioral alterations. This confirms the protective effects of low-dose MC on RGC loss in this I/R model.

DISCUSSION

In the present study, we evaluated RGC loss in I/R injury mice and found that low-dose MC can rescue RGCs based on histologic analysis, visual functional changes, and behavioral tests. Ischemia-associated retinal degeneration leads to severe visual impairment, and even blindness [46]. The ischemic retina injury model can be created with acute hypertension, where high IOP-induced injury was used in this model [47-49]. Because of the presence of ischemic impact in glaucoma and the ease of establishing a model, the I/R model has been more popularly used in studies of neurodegeneration and neuroprotection of RGCs in glaucoma studies [50]. We reported the loss of RGCs in the I/R model in a previous study [11]. In the present study, we detected less RGC loss and inner retinal layer thinning in the low-dose MC treatment group, which suggested that the loss of RGCs is induced by a transient ischemic attack, while MC has potential RGC protective properties.

A previous study showed a close relationship between microglia and RGCs in glaucoma [51]. Microglial cells were reported to be involved in the development of many neurodegenerative diseases and neurologic disorders, including glaucoma [52]. There is increasing evidence showing the detrimental effects of activated microglia, while suppressing the activation of microglia can improve the survival of RGCs [53,54]. To date, in CNS degenerative diseases, the main mechanism for the neuroprotective effect of MC has been thought due to inhibiting the activation of microglial cells [54,55]. Consistent with this, the present data showed that the number of activated microglia was reduced by treatment with low-dose MC (20 mg/kg) when compared with the vehicle-treated I/R injury group. The reduction in the number of microglia was consistent with the increased survival of RGCs in the low-dose MC group, but not in the high-dose MC group, which suggested that microglia may promote repair of the injured retina. In a recent study, we reported that microglial activation induced RGC damage [54]. Moreover, the present data also showed inhibiting microglial activity by MC had neuroprotective effects. However, high-dose MC induced toxicity toward neuron and non-neuronal retinal cells. Thus, microglia should be a key target for neuroprotection related to ischemia. The data demonstrated that MC may exert a neuroprotective role in glaucoma via suppression of microglial activation,

The OKT has been widely applied as a visual function test in mice with retinal degenerative diseases [56]. Optokinetic tasks overcome the limitations of other visual tasks, as they require no reinforcement training for measurement of vision. In the present study, the OKT analysis showed that the light-adapted visual acuity of low-dose MC-treated I/R injury mice was statistically significantly better than that of I/R injury + NS-treated group, which further suggested the neural protective features of low-dose MC.

ERG is commonly considered a more sensitive method than histology in evaluating retinal insults [57]. PhNR is dependent on the activity of RGCs and is reduced in eyes with experimental glaucoma. The present ERG data indicated that RGC function was damaged under transient ocular hypertension and protected by low-dose MC. From the onset of the waves in ERG, the a-wave is generated by photoreceptors, while the b-wave mainly originates from bipolar cells that are post-synaptic to photoreceptors. Scotopic a-waves are related to rod function, while photopic waves are related to cone function. A previous study reported that photoreceptors are damaged in glaucoma [26]. The present data showed that the average amplitude and latency time for scotopic ERG a-waves were different between the I/R injury + NS group and the low-dose MC group. Conversely, there were no statistically significant differences in the average amplitude and latency time for photopic ERG a-waves. The ERG a- and b-waves correlated with changes in the retinal layer thickness, which indicated that MC could prevent RGCs and photoreceptors from glaucomatous damage. In conclusion, the present study demonstrated the protective effects of low-dose MC on I/R injury–induced RGC loss, making MC an appealing candidate for glaucoma therapy. The possible mechanism of action is related to the inhibition of microglial activation. An equally important finding is that MC had not only dose-dependent neuroprotective effects but also potential toxicity at a high dose for neurons and non-neuronal cells. The results also indicated that MC, at appropriate doses, may be an effective therapeutic intervention for ischemic damage of the retina.

ACKNOWLEDGMENTS

The authors thank Shen Ning and Bie Man for their technical assistance.This study was supported by the Special Fund for Scientific Research and Development of the First Affiliated Hospital of Jinan University (No. 2017203),the Natural Science Foundation of China 2013 (No. 81300766) and Guangdong Provincial Medical Science Foundation (No. A2016271). Xuesong Mi (mxsong@163.com) and Yong Ding (dingyong@jnu.edu.cn) are co-corresponding authors for this paper.

REFERENCES

1. Hashem HE, Abd El-Haleem MR, Amer MG, Bor'i A. Pomegranate protective effect on experimental ischemia/reperfusion retinal injury in rats (histological and biochemical study). Ultrastruct Pathol 2017; 41:346-57. [PMID: 28796566].
2. Quigley HA, Nickells RW, Kerrigan LA, Pease ME, Thibault DJ, Zack DJ. Retinal ganglion cell death in experimental glaucoma and after axotomy occurs by apoptosis. Invest Ophthalmol Vis Sci 1995; 36:774-86. [PMID: 7706025].
3. Gupta N, Yucel YH. Glaucoma as a neurodegenerative disease. Curr Opin Ophthalmol 2007; 18:110-4. [PMID: 17301611].
4. Lee DA, Higginbotham EJ. Glaucoma and its treatment: a review. Am J Health Syst Pharm 2005; 62:691-9. [PMID: 15790795].
5. Almasieh M, Wilson AM, Morquette B, Cueva Vargas JL, Di Polo A. The molecular basis of retinal ganglion cell death in glaucoma. Prog Retin Eye Res 2012; 31:152-81. [PMID: 22155051].
6. Gonzalez Fleitas MF, Bordone M, Rosenstein RE, Dorfman D. Effect of retinal ischemia on the non-image forming visual system. Chronobiol Int 2015; 32:152-63. [PMID: 25238585].
7. Della Santina L, Inman DM, Lupien CB, Horner PJ, Wong RO. Differential progression of structural and functional alterations in distinct retinal ganglion cell types in a mouse model of glaucoma. J Neurosci 2013; 33:17444-57. [PMID: 24174678].
8. Mi XS, Feng Q, Lo AC, Chang RC, Lin B, Chung SK, So KF. Protection of retinal ganglion cells and retinal vasculature by Lycium barbarum polysaccharides in a mouse model of acute ocular hypertension. PLoS One 2012; 7:e45469-[PMID: 23094016].
9. Kim SY, Shim MS, Kim KY. Weinreb RN1 Wheeler LA, Ju WK1. Inhibition of cyclophilin D by cyclosporin A promotes retinal ganglion cell survival by preventing mitochondrial alteration in ischemic injury. Cell Death Dis 2014; 5:e1105-[PMID: 24603333].
10. Bosco A, Romero CO, Breen KT, Chagovetz AA, Steele MR, Ambati BK, Vetter ML. Neurodegeneration severity can be predicted from early microglia alterations monitored in vivo in a mouse model of chronic glaucoma. Dis Model Mech 2015; 8:443-55. [PMID: 25755083].
11. Zhu S, Stavrovskaya IG, Drozda M, Kim BY, Ona V, Li M, Sarang S, Liu AS, Hartley DM, Wu DC, Gullans S, Ferrante RJ, Przedborski S, Kristal BS, Friedlander RM. Minocycline inhibits cytochrome c release and delays progression of amyotrophic lateral sclerosis in mice. Nature 2002; 417:74-8. [PMID: 11986668].
12. Xu L, Fagan SC, Waller JL, Edwards D, Borlongan CV, Zheng J, Hill WD, Feuerstein G, Hess DC. Low dose intravenous minocycline is neuroprotective after middle cerebral artery occlusion-reperfusion in rats. BMC Neurol 2004; 4:7-[PMID: 15109399].
13. Tao T, Xu G, Si Chen C, Feng J, Kong Y, Qin X. Minocycline promotes axonal regeneration through suppression of RGMa in rat MCAO/reperfusion model. Synapse 2013; 67:189-98. [PMID: 23184880].
14. Choi Y, Kim HS, Shin KY, Kim EM, Kim M, Kim HS, Park CH, Jeong YH, Yoo J, Lee JP, Chang KA, Kim S, Suh YH. Minocycline attenuates neuronal cell death and improves cognitive impairment in Alzheimer's disease models. Neuropsychopharmacology 2007; 32:2393-404. [PMID: 17406652].
15. Seidl SE, Potashkin JA. The promise of neuroprotective agents in Parkinson's disease. Front Neurol 2011; 2:68-[PMID: 22125548].
16. Chen X, Chen S, Jiang Y, Zhu C, Wu A, Ma X, Peng F, Ma L, Zhu D, Wang Q, Pi R. Minocycline reduces oxygen-glucose deprivation-induced PC12 cell cytotoxicity via matrix metalloproteinase-9, integrin beta1 and phosphorylated Akt modulation. Neurol Sci 2013; 34:1391-6. [PMID: 23224583].
17. Wang X, Zhu S, Drozda M, Zhang W, Stavrovskaya IG, Cattaneo E, Ferrante RJ, Kristal BS, Friedlander RM. Minocycline inhibits caspase-independent and -dependent mitochondrial cell death pathways in models of Huntington's disease. Proc Natl Acad Sci USA 2003; 100:10483-7. [PMID: 12930891].
18. Wu Y, Chen Y, Wu Q, Jia L, Du X. Minocycline inhibits PARP1 expression and decreases apoptosis in diabetic retinopathy. Mol Med Rep 2015; 12:4887-94. [PMID: 26165350].
19. Ferrer-Martín RM, Martín-Oliva D, Sierra-Martín A, Carrasco MC, Martín-Estebané M, Calvente R, Martín-Guerrero SM, Marín-Teva JL, Navascués J, Cuadros MA. Microglial Activation Promotes Cell Survival in Organotypic Cultures of Postnatal Mouse Retinal Explants. PLoS One 2015; 10:e0135238-.
20. Abcouwer SF, Lin CM, Shanmugam S, Muthusamy A, Barber AJ, Antonetti DA. Minocycline prevents retinal inflammation and vascular permeability following ischemia-reperfusion injury. J Neuroinflammation 2013; 10:149-.
21. Chen YI, Lee YJ, Wilkie DA, Lin CT. Evaluation of potential topical and systemic neuroprotective agents for ocular hypertension-induced retinal ischemia-reperfusion injury. Vet Ophthalmol 2014; 17:432-42. [PMID: 24171811].
22. Levkovitch-Verbin H, Waserzoog Y, Vander S, Makarovsky D, Piven I. Minocycline upregulates pro-survival genes and downregulates pro-apoptotic genes in experimental glaucomaGraefes. Arch Clin Exp Ophthalmol 2014; 252:761-72. [PMID: 24566901].
23. Peng B, Xiao J, Wang K, So KF, Tipoe GL, Lin B. Suppression of microglial activation is neuroprotective in a mouse model of human retinitis pigmentosa. J Neurosci 2014; 34:8139-50. [PMID: 24920619].
24. Wu Y, Chen Y, Wu Q, Jia L, Du X. Minocycline inhibits PARP1 expression and decreases apoptosis in diabetic retinopathy. Mol Med Rep 2015; 12:4887-94. [PMID: 26165350].
25. Halder SK, Matsunaga H, Ishii KJ, Ueda H. Prothymosin-alpha preconditioning activates TLR4-TRIF signaling to induce protection of ischemic retina. J Neurochem 2015; 135:1161-77. [PMID: 26364961].

26. Xu W, Yin J, Sun L, Hu Z, Dou G, Zhang Z, Wang H, Guo C, Wang Y. Impact of minocycline on vascularization and visual function in an immature mouse model of ischemic retinopathy. Sci Rep 2017; 7:7535-.

27. Karlstetter M, Scholz R, Rutar M, Wong WT, Provis JM, Langmann T. Retinal microglia: just bystander or target for therapy? Prog Retin Eye Res 2015; 45:30-57. [PMID: 25476242].

28. Gallego BI, Salazar JJ, de Hoz R, Rojas B, Ramírez AI, Salinas-Navarro M, Ortín-Martínez A, Valiente-Soriano FJ, Avilés-Trigueros M, Villegas-Perez MP, Vidal-Sanz M, Triviño A, Ramírez JM. IOP induces upregulation of GFAP and MHC-II and microglia reactivity in mice retina contralateral to experimental glaucoma. J Neuroinflammation 2012; 9:92-[PMID: 22583833].

29. Carson MJ. Microglia as liaisons between the immune and central nervous systems: functional implications for multiple sclerosis. Glia 2002; 40:218-31. [PMID: 12379909].

30. Karlstetter M, Scholz R, Rutar M, Wong WT, Provis JM. Langmann T4. Retinal microglia: just bystander or target for therapy? Prog Retin Eye Res 2015; 45:30-57. [PMID: 25476242].

31. Velten IM, Korth M, Horn FK. The a-wave of the dark adapted electroretinogram in glaucomas: are photoreceptors affected? Br J Ophthalmol 2001; 85:397-402. [PMID: 11264126].

32. Ortín-Martínez A, Salinas-Navarro M, Nadal-Nicolás FM, Jiménez-López M, Valiente-Soriano FJ, García-Ayuso D, Bernal-Garro JM, Avilés-Trigueros M, Agudo-Barriuso M, Villegas-Pérez MP, Vidal-Sanz M. Laser-induced ocular hypertension in adult rats does not affect non-RGC neurons in the ganglion cell layer but results in protracted severe loss of cone-photoreceptors. Exp Eye Res 2015; 132:17-33. [PMID: 25576772].

33. Diehl KH, Hull R, Morton D, Pfister R, Rabemampianina Y, Smith D, Vidal JM, van de Vorstenbosch C. European Federation of Pharmaceutical Industries Association and European Centre for the Validation of Alternative Methods. A good practice guide to the administration of substances and removal of blood, including routes and volumes. J Appl Toxicol 2001; 21:15-23. [PMID: 11180276].

34. Galindo-Romero C, Jimenez-Lopez M, Garcia-Ayuso D, Salinas-Navarro M, Nadal-Nicolás FM, Agudo-Barriuso M, Villegas-Pérez MP, Avilés-Trigueros M, Vidal-Sanz M. Number and spatial distribution of intrinsically photosensitive retinal ganglion cells in the adult albino rat. Exp Eye Res 2013; 108:84-93. [PMID: 23295345].

35. Nadal-Nicolas FM, Salinas-Navarro M, Jimenez-Lopez M, Sobrado-Calvo P, Villegas-Pérez MP, Vidal-Sanz M, Agudo-Barriuso M. Displaced retinal ganglion cells in albino and pigmented rats. Front Neuroanat 2014; 8:99-[PMID: 25339868].

36. Galindo-Romero C, Valiente-Soriano FJ, Jimenez-Lopez M, García-Ayuso D, Villegas-Pérez MP, Vidal-Sanz M, Agudo-Barriuso M. Effect of brain-derived neurotrophic factor on mouse axotomized retinal ganglion cells and phagocytic microglia. Invest Ophthalmol Vis Sci 2013; 54:974-85. [PMID: 23307961].

37. Redfern WS, Storey S, Tse K, Hussain Q, Maung KP, Valentin JP, Ahmed G, Bigley A, Heathcote D, McKay JS. Evaluation of a convenient method of assessing rodent visual function in safety pharmacology studies: effects of sodium iodate on visual acuity and retinal morphology in albino and pigmented rats and mice. J Pharmacol Toxicol Methods 2011; 63:102-14. [PMID: 20619348].

38. Prusky GT, Alam NM, Beekman S, Douglas RM. Rapid quantification of adult and developing mouse spatial vision using a virtual optomotor system. Invest Ophthalmol Vis Sci 2004; 45:4611-6. [PMID: 15557474].

39. Yang S, Luo X, Xiong G, So KF, Yang H, Xu Y. The electroretinogram of Mongolian gerbil (Meriones unguiculatus): Comparison to mouse. Neurosci Lett 2015; 589:7-12. [PMID: 25578951].

40. Luo X, Yu Y, Xiang Z, Wu H, Ramakrishna S, Wang Y, So KF, Zhang Z, Xu Y. Tetramethylpyrazine nitrone protects retinal ganglion cells against N-methyl-D-aspartate-induced excitotoxicity. J Neurochem 2017; 141:373-86. [PMID: 28160291].

41. Shen N, Qu Y, Yu Y, So KF, Goffinet AM, Vardi N, Xu Y, Zhou L. Frizzled3 Shapes the Development of Retinal Rod Bipolar Cells. Invest Ophthalmol Vis Sci 2016; 57:2788-96. .

42. Yun H, Lathrop KL, Yang E, Sun M, Kagemann L, Fu V, Stolz DB, Schuman JS, Du Y. A laser-induced mouse model with long-term intraocular pressure elevation. PLoS One 2014; 9:e107446-[PMID: 25216052].

43. Bosco A, Inman DM, Steele MR, Wu G, Soto I, Marsh-Armstrong N, Hubbard WC, Calkins DJ, Horner PJ, Vetter ML. Reduced retina microglial activation and improved optic nerve integrity with minocycline treatment in the DBA/2J mouse model of glaucoma. Invest Ophthalmol Vis Sci 2008; 49:1437-46. [PMID: 18385061].

44. Cahill H, Nathans J. The optokinetic reflex as a tool for quantitative analyses of nervous system function in mice: application to genetic and drug-induced variation. PLoS One 2008; 3:e2055-[PMID: 18446207].

45. Nucci C, Tartaglione R, Rombolà L, Morrone LA, Fazzi E, Bagetta G. Neurochemical evidence to implicate elevated glutamate in the mechanisms of high intraocular pressure (IOP)-induced retinal ganglion cell death in rat. Neurotoxicology 2005; 26:935-41. [PMID: 16126273].

46. Mathew B, Poston JN, Dreixler JC, Torres L, Lopez J, Zelkha R, Balyasnikova I. Lesniak MS4, Roth S. Bone-marrow mesenchymal stem-cell administration significantly improves outcome after retinal ischemia in rats. Graefes Arch Clin Exp Ophthalmol 2017; 255:1581-92. [PMID: 28523456].

47. de Hoz R, Gallego BI, Ramírez AI, Rojas B, Salazar JJ, Valiente-Soriano FJ, Avilés-Trigueros M, Villegas-Perez MP, Vidal-Sanz M, Triviño A, Ramírez JM. Rod-like microglia are restricted to eyes with laser-induced ocular hypertension but absent from the microglial changes in the contralateral untreated eye. PLoS One 2013; 8:e83733-[PMID: 24367610].

48. Renner M, Stute G, Alzureiqi M, Reinhard J, Wiemann S, Schmid H, Faissner A, Dick HB, Joachim SC. Optic Nerve Degeneration after Retinal Ischemia/Reperfusion in a Rodent Model. Front Cell Neurosci 2017; 11:254-[PMID: 28878627].

49. Rovere G, Nadal-Nicolas FM, Wang J, Bernal-Garro JM, García-Carrillo N, Villegas-Pérez MP, Agudo-Barriuso M, Vidal-Sanz M. Melanopsin-Containing or Non-Melanopsin-Containing Retinal Ganglion Cells Response to Acute Ocular Hypertension With or Without Brain-Derived Neurotrophic Factor Neuroprotection. Invest Ophthalmol Vis Sci 2016; 57:6652-61. [PMID: 27930778].

50. Trost A, Motloch K, Bruckner D, Schroedl F, Bogner B, Kaser-Eichberger A, Runge C, Strohmaier C, Klein B, Aigner L, Reitsamer HA. Time-dependent retinal ganglion cell loss, microglial activation and blood-retina-barrier tightness in an acute model of ocular hypertension. Exp Eye Res 2013; 136:59-71. [PMID: 26001526].

51. Rojas B, Gallego BI, Ramírez AI, Salazar JJ, de Hoz R, Valiente-Soriano FJ, Avilés-Trigueros M, Villegas-Perez MP, Vidal-Sanz M, Triviño A, Ramírez JM. Microglia in mouse retina contralateral to experimental glaucoma exhibit multiple signs of activation in all retinal layers. J Neuroinflammation 2014; 11:133-[PMID: 25064005].

52. Yang F, Wu L, Guo X, Wang D, Li Y. Improved retinal ganglion cell survival through retinal microglia suppression by a chinese herb extract, triptolide, in the DBA/2J mouse model of glaucoma. Ocul Immunol Inflamm 2013; 21:378-89. [PMID: 23876132].

53. Lujia Y, Xin L, Shiquan W, Yu C, Shuzhuo Z, Hong Z. Ceftriaxone pretreatment protects rats against cerebral ischemic injury by attenuating microglial activation-induced IL-1beta expression. Int J Neurosci 2014; 124:657-65. [PMID: 24985046].

54. Wang N, Mi X, Gao B, Gu J, Wang W, Zhang Y, Wang X. Minocycline inhibits brain inflammation and attenuates spontaneous recurrent seizures following pilocarpine-induced status epilepticus. Neuroscience 2015; 287:144-56. [PMID: 25541249].

55. Zhu F, Zheng Y, Liu Y, Zhang X, Zhao J. Minocycline alleviates behavioral deficits and inhibits microglial activation in the offspring of pregnant mice after administration of polyriboinosinic-polyribocytidilic acid. Psychiatry Res 2014; 219:680-6. [PMID: 25042426].

56. Burroughs SL, Kaja S, Koulen P. Quantification of deficits in spatial visual function of mouse models for glaucoma. Invest Ophthalmol Vis Sci 2011; 52:3654-9. [PMID: 21330670].

57. Rösch S, Johnen S, Müller F, Pfarrer C, Walter P. Correlations between ERG, OCT, and Anatomical Findings in the rd10 Mouse. J Ophthalmol 2014; xxx:874751-.

Articles are provided courtesy of Emory University and the Zhongshan Ophthalmic Center, Sun Yat-sen University, P.R. China. The print version of this article was created on 18 May 2018. This reflects all typographical corrections and errata to the article through that date. Details of any changes may be found in the online version of the article.